Published in final edited form as:
Magn Reson Med. 2005 November ; 54(5): 1100–1106.

High-Resolution SSFP Coronary MRA within a Breath-Hold: Parallel Imaging with Extended Cardiac Data Acquisition

Jaeseok Park[1,2], **Andrew C. Larson**[1], **Qiang Zhang**[3], **Orlando Simonetti**[3], and **Debiao Li, PhD**[1,2]

1 *Department of Radiology, Northwestern University, Chicago, Illinois, USA,*

2 *Department of Biomedical Engineering, Chicago, Illinois, USA,*

3 *Siemens Medical Solutions, Chicago, Illinois, USA*

Abstract

Coronary artery imaging data is conventionally acquired in a single imaging frame during mid-diastole. Data acquisition window must be sufficiently short to avoid cardiac motion artifacts. The short data acquisition window results in decreased imaging efficiency and limited spatial resolution. Parallel imaging may lessen these limitations, but requires highly accurate coil sensitivity.

The purpose of this work was to increase the imaging efficiency and spatial resolution in coronary artery imaging using parallel imaging with extended acquisition window. External coil calibration data were acquired before and after a short mid-diastolic period of accelerated imaging data acquisition. It was assumed that residual cardiac motion in the extended acquisition window would not impede accurate estimation of coil sensitivity since only low spatial frequency signals were acquired for coil calibration. Experimental studies were performed in 5 healthy volunteers at 3T using steady state free precession sequence. Statistical comparison was made between the proposed method and conventional data acquisition for visual quality of image and vessel sharpness. The proposed technique demonstrated higher visual grading (2.1±0.32 vs. 3.4±0.52, P=0.00017) and improved vessel sharpness (0.61±0.024 vs. 0.88±0.072, P=0.0000056). The proposed method is a new approach to enhance the imaging efficiency and spatial resolution in coronary artery imaging.

Keywords

Magnetic Resonance Imaging (MRI); Coronary MRA; Parallel MRI; Rapid Imaging; SSFP

INTRODUCTION

In coronary magnetic resonance angiography (MRA), data is conventionally acquired in a single frame during mid-diastole. The data acquisition window must be sufficiently short to avoid cardiac motion artifacts. The short data acquisition window results in decreased imaging efficiency, limiting spatial resolution or three-dimensional (3D) volume coverage for breath-hold coronary MRA.

Partially parallel acquisition techniques (1–9) offer the potential to overcome the aforementioned limitations in coronary MRA, using arrays of multiple receiver coils. Coil k-

Please send correspondence and reprint requests to: Debiao Li, PhD, 448 East Ontario Street, Suite 700, Chicago, IL 60611, Tel: (312) 926-4245, Fax: (312) 896-5665, E-mail: d-li2@northwestern.edu.

Supported in part by a National Institutes of Health Grant (no. EB002623 and HL38698) and by Siemens Medical Solutions, Malvern, PA, USA

space is under-sampled in the phase encoding (PE) direction as compared to conventional data acquisition. These techniques exploit the knowledge of spatial coil sensitivity to generate a fully reconstructed image from the under-sampled data. Coil sensitivity is conventionally calculated by either external or internal coil calibration. For the external coil calibration (1–5), a low-resolution image is typically acquired in a separate scan from accelerated imaging data. However, this strategy does not ensure that coil and cardiac positions are exactly the same during coil calibration and the accelerated imaging scan. Coil calibration errors may result in residual aliasing artifact and noise amplification in image reconstruction. For the internal coil calibration (6–9), calibration signals are additionally acquired in the central k-space of accelerated data using variable density (VD) sampling in the PE direction. Although the VD accelerated sampling scheme minimizes calibration errors resulting from coil or cardiac motion, the additional calibration signals sampled in the central k-space may place limits on achievable spatial resolution.

The hypothesis of this work was that the imaging efficiency and spatial resolution in coronary MRA could be increased with no apparent motion artifacts using parallel imaging with extended acquisition window. External calibration data were acquired before and after a short mid-diastolic period of accelerated imaging data acquisition in a single measurement. It was assumed that residual cardiac motion in the extended acquisition window would not impede the accurate estimation of coil sensitivity map because only low spatial frequency signals were acquired for coil calibration. Experimental studies were performed in volunteers at 3T using steady state free precession (SSFP) sequence to validate this technique. The proposed method is a new simple approach to achieve high spatial resolution in coronary artery imaging.

THEORY

Extended Data Acquisition and Coil Calibration

A schematic of the proposed extended data acquisition and view ordering scheme is shown in Figure 1 using three imaging frames acquired around cardiac mid-diastole. A spectrally selective fat saturation pulse was first applied. SSFP data acquisition was preceded by the application of five dummy radio frequency (RF) pulses with sinusoidally varying flip angles (12) for a smooth transition to steady state. Data were under-sampled with a reduction factor (R) of three in the 2^{nd} imaging frame, while missing low frequency lines were acquired in the 1^{st} and 3^{rd} imaging frames for external calibration data (Fig. 1a). The under-sampled data within a specified low-frequency range was combined with the external calibration data for coil calibration. The combined k-space was zero padded, and then Fourier transformed to yield each coil image. These images were normalized by the root sum of squared magnitudes of all the coil images, generating coil sensitivity images. If the number of PE lines in calibration region (= N^{CAL}) is too small, Gibbs ringing artifact may result, which is then modulated somewhat differently for each coil. The artifact-induced errors in coil calibration may cause severe artifacts in reconstructed images. It is, therefore, necessary to determine the optimal ratio (= R_1) of NCAL to the total number of reconstructed PE lines (= N^{PE}).

To effectively suppress epicardial fat signals around coronary arteries, the under-sampled data in the 2^{nd} imaging frame was acquired from the low to high frequencies using centric reordering in the PE direction (Fig. 1c). For reduction of signal discontinuity in the central region of the combined k-space in coil calibration due to SSFP signal transition, the external calibration lines were acquired from the high to low frequencies in the 1^{st} imaging frame (Fig. 1b), and from a certain frequency to higher frequencies in the 3^{rd} imaging frame (Fig. 1d). The ratio (= R_2) of the number of PE lines within a specified cutoff frequency (= N^{CUTOFF}) to N^{CAL} needs to be determined to minimize coil calibration errors which may result from the signal discontinuity of combined k-space. In addition, to reduce eddy-current induced artifacts in coil calibration,

PE lines in the neighborhood of k-space were acquired with an alternating RF phase (Figs. 1b-d) using double cycling with balanced SSFP (13).

Image Reconstruction

Images were reconstructed from the under-sampled data acquired in the 2nd imaging frame using a parallel imaging technique, generalized simultaneous acquisition of spatial harmonics (GSMASH) (1). GSMASH reconstruction is, however, susceptible to severe signal loss and noise amplification at high acceleration factor. In this work, GSMASH reconstruction was modified to incorporate regularization method (14) to reduce noise.

The MR imaging signal is represented by the following equation:

$$S_l(x, k_y) = \int dy\ C_l(x, y)\rho(x, y)e^{-jk_y y} \quad [1]$$

where l is a coil index, $S_l(x, k_y)$ is a signal acquired after Fourier transforming coil k-space in the readout direction, $C_l(x, y)$ is coil sensitivity, and $\rho(x, y)$ is a complex image value. In GSMASH, coil sensitivity is approximated using linear superposition of a number of spatial harmonic profiles:

$$C_l(x, y) = \sum_{m=-p}^{q} a_l^m(x)e^{-jm\Delta k_y y} \quad [2]$$

$$a_l^m(x) = \left[a_l^{-p} a_l^{-p+1} \cdots \cdots a_l^q\right] = DFT_y[C_l(x, y)] \quad [3]$$

where m is the m^{th} order of spatial harmonic, $-p$ is the minimum order of spatial harmonic, q is the maximum order of spatial harmonic, and $a_l^m(x)$ is calculated by discrete Fourier transform (DFT) of coil sensitivity in y direction. Inserting Eq. [2] into Eq. [1], the MR signal Eq. [1] is then changed to:

$$S_l(x, k_y) = \sum_{m=-p}^{q} a_l^m(x)\int dy\rho(x, y)e^{-j(k_y+m\Delta k_y)y} \quad [4]$$

In this work, Eq. [4] is approximated using a discrete form by the following equations to be compatible with a general framework of parallel imaging (5):

$$S_l(x, k_y) \approx \sum_m a_l^m(x)\sum_y e^{-j(k_y+m\Delta k_y)y}\rho(x, y) \quad [5]$$

$$S_l \approx A_l E_{k_y}\rho \quad [6]$$

where A_l (matrix = 1 x N^{PE}) is the Fourier coefficient matrix made of $a_l^m(x)$, E_{ky} (matrix = N^{PE}x N^{PE}) is the encoding matrix composed of spatial harmonic profiles. To consider the signal periodicity in k-space along the PE direction, the encoding matrix is reconstructed by:

$$E_{k_y} = DFT_{column}(Id_{k_y}) \quad [7]$$

$$Id_{k_y} = \begin{cases} \begin{bmatrix} I_{N^{PE}} \end{bmatrix} & , k_y = 0 \\ \begin{bmatrix} 0 & I_{N^{PE}-k_y} \\ I_{k_y} & 0 \end{bmatrix} & , k_y = 1, 2, \cdots \cdots \end{cases} \quad [8]$$

where Id_{ky} is an N^{PE}x N^{PE} identity matrix circularly rotating in the row direction with k_y, and I_N is an N by N identity matrix.

Including the data acquired over all the coils, Eq. [6] is written as:

$$S_{Measured} \approx AE\rho = B\rho \quad [9]$$

To reduce noise amplification from an ill-conditioned direct inversion in Eq. [9], the solution can be expressed using Tikhonov regularization as (14):

$$\rho = \min_{\rho} \left\{ \| B\rho - S_{Measured} \|_2 + \lambda^2 \| \rho - \rho^0 \|_2 \right\} \quad [10]$$

where λ is a regularization parameter, ρ^0 is the prior information about the solution ρ, and $\| \cdot \|_2$ represents the matrix 2-norm. The prior information, ρ^0, in this work is obtained by conventional GSMASH reconstruction using the k-space combined for coil calibration. GSMASH with regularization yields an intermediate solution between direct inversion (= $B^{-1} S_{Measured}$) and ρ^0, providing a tradeoff between image accuracy and noise.

Materials and Methods

Data acquisition was performed in five healthy volunteers and a phantom using 3D segmented SSFP sequence on a 3 T whole body MR scanner (MAGNETOM Trio, Siemens Medical Solutions, Erlangen, Germany) equipped with a high performance gradient sub-system (maximum amplitude: 40 mT/m, maximum slew rate: 200 mT/m/ms). An informed written consent was obtained from each volunteer before the study, and was approved by our Institutional Review Board. During each scan, the volunteers were instructed to hold their breaths at the end of inspiration. An array of 8-element rectangular surface coil (dimension of coil element: 11 x 12 cm^2) was placed anterior (6 coil elements) and posterior (2 coil elements) to a subject. The anterior coil array was composed of two elements along the body axis and three elements along the left-right direction, and the posterior array consisted of two elements along the body axis. The internal rectangular coil elements were overlapped to null the mutual inductance between neighboring coil elements. Image reconstruction was implemented in the Matlab software package (MathWorks, Natick, MA). The common imaging parameters were as follows: TR (time of repetition) / TE (time of echo) / flip angle = 3.6 ms/1.8ms/40–50°, FOV (field-of-view) = 250 x 350 mm^2, number of partitions = 6 (interpolated to 12), slice thickness = 3mm (interpolated to 1.5 mm), number of heartbeats / partition = 4, and breath-hold duration = 16–24 sec. The imaging protocols were within the limit of the specific energy absorption rate (SAR) approved by FDA.

Optimization of Acquisition Parameters

To determine the ratio R_1 for Gibbs ringing artifact reduction in coil calibration, a set of left anterior descending (LAD) artery data was fully acquired in one volunteer with conventional acquisition (matrix = 300x448, 30 lines/heartbeat (HB)), and then decimated with R = 3. A reference image was generated by GSMASH reconstruction with the fully acquired data. The reduced data was reconstructed by conventional GSMASH and regularized GSMASH as the ratio R_1 varies. The regularization parameter, λ, was chosen to be 5.0. The parameter, λ , can

be automatically determined as (15), but in this work, is fixed to an empirically determined constant value. Artifact power (AP) was calculated with R_1 by:

$$AP = \frac{\sum_j \left| \left| I_j^{reference} \right|^2 - \left| I_j^{reconstructed} \right|^2 \right|}{\sum_j \left| I_j^{reference} \right|^2} \quad [11]$$

where j is the index of image pixel, $I^{reference}$ is a reference image, and $I^{reconstructed}$ is a reconstructed image.

Several sets of data were acquired in a phantom using the proposed extended acquisition with different ratios of R_2 to investigate the effect of SSFP signal discontinuity of k-space on coil sensitivity estimation. The ratio of R_1 was fixed to 0.4 at which the AP was changed slowly around its minimal value, based on results in the next section. Coil sensitivity was reconstructed using the combined k-space acquired for coil calibration. A reference data was fully acquired using linear reordering of PE lines to minimize the signal discontinuity in k-space, and then coil sensitivity was reconstructed. AP was calculated to determine an optimal ratio R_2, measuring the signal discontinuity of the combined k-space in coil calibration. A phantom was used to determine R_2 because it is difficult to obtain an accurate AP due to motion with in vivo data.

To demonstrate the effectiveness of the proposed method using the determined parameters of R_1 and R_2, three sets of 3D coronary artery data were acquired in each volunteer (RR interval ranges from 650 ms to 1000 ms) during the same imaging time using: 1) conventional data acquisition with a short window (duration = 127 ms, matrix = 140 x 448, 35 lines/HB), 2) conventional data acquisition with an extended window (duration = 270 ms, matrix = 300 x 448, 75 lines / HB), and 3) the proposed data acquisition (duration = 162 ms (1^{st} imaging frame = 36 ms, 2^{nd} imaging frame = 90 ms, and 3^{rd} imaging frame = 36 ms), matrix = 100 x 448 and 25 lines / HB for the 2^{nd} imaging frame, matrix = 40 x 448 and 10 lines / HB for the 1^{st} and 3^{rd} imaging frames, respectively). The three data acquisitions have the same imaging time (= 16–24 sec due to different RR intervals) and 6 partitions (interpolated to 12).

Analysis

The images reconstructed using the three different data acquisitions mentioned above were combined with randomized ordering in a single viewing slide, and then visually graded by the two reviewers (experienced in coronary MRA) who were not involved in the study. The visual grading was based on a 4-point scale: 1) poor (severe blurring), 2) fair (moderate blurring), 3) good (mild blurring), and 4) excellent (sharp vessel definition). The vessel sharpness was estimated using the intensity profile (similar to Gaussian profile) along the user-specified proximal coronary segments with a public domain image processing software (Scion Image, Release Beta 3b, Scion Corporation, Frederick, MD) (16). The distance between 20 and 80 % of maximum intensity was measured for each side of the profile, and then averaged. The reciprocal of the averaged distance was taken as sharpness. Qualitative image scores and quantitative vessel sharpness measurements were statistically evaluated by a one-factor analysis of variance (ANOVA) with P-value of 0.05.

RESULT

Figure 2 shows AP and the corresponding images generated using conventional and regularized GSMASH reconstruction with the increase of R_1 (R = 3). AP decreases rapidly until R_1 reaches around 0.3, and then reduces slowly with $R_1 > 0.3$ (Fig. 2a). The regularized GSMASH yields an AP lower than half that of conventional GSMASH with R_1. In conventional GSMASH, severe artifact and amplified noise is observed when R_1 is small (Fig. 2c) as compared to a

reference (Fig. 2b). As R_1 is increased, residual artifacts are reduced (arrows), but noise remains severe (Figs. 2d, 2e). In regularized GSMASH, noise is decreased over all the ranges of R_1, but image blurring is observed at $R_1 = 0.15$ (Fig. 2f). As R_1 is increased, image accuracy is improved (Figs. 2g, 2h).

Figure 3 demonstrates AP (Fig. 3a) and the corresponding coil sensitivity images (Figs. 3b–f) with the increase of R_2 ($R_1 = 0.4$) in the proposed data acquisition to investigate the effect of signal discontinuity in the combined k-space on coil sensitivity estimation. AP is rapidly decreased until R_2 reaches around 0.4, representing that signal discontinuity is reduced in the low-frequency region of the combined k-space for coil calibration. AP remains nearly identical with $R_2 > 0.4$. Compared to the reference (Fig. 3b), the signal discontinuity related artifacts are severe at $R_2 = 0.04$ (Fig. 3c) and 0.20 (Fig. 3d), but are reduced much at $R_2 = 0.36$ (Fig. 3e) and 0.84 (Fig. 3f).

Figure 4 shows the effectiveness of the proposed method with the optimal parameters of R_1 and R_2 as compared to conventional data acquisition. An image acquired with conventional single frame mid-diastolic data acquisition with a short window (= 127 ms) results in low spatial resolution (Figs. 4a, 4b). Extending the data acquisition window (= 270 ms) enhances spatial resolution, but is susceptible to motion-induced vessel blurring or artifacts (Figs. 4c, 4d). The proposed data acquisition (window duration = 162 ms, $R_1 = 0.4$, $R_2 = 0.5$, $R = 3$) with regularized GSMASH reconstruction ($\lambda = 5.0$) yields high spatial resolution with reduced motion artifacts (Figs. 4e, 4f). In extending the data acquisition window, motion artifacts are more severe with a short RR interval (Fig. 4d) than with a long RR interval (Fig. 4c).

In five volunteers, the above three data acquisition methods show statistically significant differences in qualitative visual grading ($P = 0.00017$) and quantitative vessel sharpness ($P = 0.0000056$). Compared with the conventional data acquisition, the proposed method demonstrates higher visual grading (conventional acquisition with a short window = 2.1 ± 0.32, conventional extended acquisition = 2.5 ± 0.84, and proposed acquisition = 3.4 ± 0.52) and improved vessel sharpness (conventional acquisition with a short window = 0.61 ± 0.024, conventional extended acquisition = 0.79 ± 0.044, and proposed acquisition = 0.88 ± 0.072).

DISCUSSION

The proposed extended data acquisition with regularized GSMASH reconstruction for coronary artery imaging has been successfully demonstrated, providing enhanced imaging efficiency and spatial resolution with nearly no motion-induced artifacts.

Extending the data acquisition window in coronary MRA to increase imaging efficiency typically results in the following two problems: cardiac motion and fat signal recovery following frequency selective fat saturation preparation pulse.

One method to resolve the motion problem for SSFP data acquisition is to utilize radial or spiral k-space sampling trajectories (17,18) that are inherently less sensitive to motion artifacts because of low-frequency averaging effects. However, radial or spiral k-space acquisition with SSFP at 3T is highly sensitive to B_0-inhomogeneity, potentially resulting in either severe banding artifacts or image blurring. Furthermore, radial and spiral sampling techniques are less compatible with centric reordering strategies for effective fat suppression following a saturation pulse. In the proposed scheme, only the accelerated data in the 2^{nd} imaging frame (90 ms in cardiac mid-diastole) is included in image reconstruction, reducing motion-induced artifacts by using a short effective acquisition window, while the external calibration data in the 1^{st} and 3^{rd} imaging frames are employed only for calculating coil sensitivity.

To suppress fat signals effectively in conventional extended acquisitions (19), a spectrally selective fat saturation pulse needs to be applied periodically during data acquisition. However, this approach interrupts steady state data acquisition, and may yield transient artifacts in reconstructed images. An alternative method involves using a specific range of TR with SSFP, making fat and water signals out-of-phase (19,20), and then removing fat signals retrospectively with phase detection. A drawback of this technique is that signals interfere destructively at the boundary between coronary artery and epicardial fat, resulting in an apparent decrease of vessel lumen size. To overcome the above limitations, the proposed method minimizes the number of dummy RF pulses with sinusoidally varying flip angles (12) as well as the number of PE lines in the 1st calibration imaging frame after spectrally selective fat saturation. In this work, only fifteen RF pulses were applied between the fat saturation pulse and the accelerated data acquisition in the 2nd imaging frame. As a result, the proposed approach should result in a similar evolution of fat signal to that expected following the fat saturation pulse in conventional short acquisition window coronary MRA (21). Further studies are needed to fully evaluate the performance of fat suppression.

In GSMASH, coil calibration is performed in image domain while reconstruction is performed in k-space. If coil calibration employs the data acquired separately from an accelerated imaging scan (2), it is prone to calibration errors due to mismatch between coil and cardiac position. In the proposed method, the accelerated imaging data within a specified frequency range are included in coil calibration, reducing the mismatch errors. In addition, the data in the proposed method are inherently acquired with VD sampling scheme within the extended acquisition window. If cardiac motion is not severe during the data acquisition, GSMASH can provide the flexibility of including the Nyquist sampled central PE lines in reconstruction process to enhance artifact suppression, since the reconstruction is performed in k-space. This flexibility is an advantage in k-space based parallel imaging techniques with VD sampling (1,5–8) as compared to image based parallel imaging techniques (2).

Direct matrix inversion in GSMASH may result in ill conditioning, which makes the large linear system underdetermined. The matrix *B* in Eq. [9] contains redundant information, and its singular value decomposition generates very small singular values. In the inversion process, the small singular values are inverted, resulting in amplified noise. The Tikhonov regularization is equivalent to applying filtering to the singular values, reducing noise. A regularized solution is an intermediate image between the direct-inversion-based image and a low-resolution reference image, yielding a tradeoff between image accuracy and noise. This proves the fact that image accuracy is improved with the increase of R_1 in Figure 2 under the same regularization parameter, since spatial resolution of the reference image is proportional to R_1. The ratio R_1 is, therefore, related to both a residual artifact level and the image accuracy in reconstructed images.

The value of R_2 was determined using phantom experiments to reduce the artifacts resulting from signal discontinuity in the combined k-space for coil calibration. However, the optimal R_2 used for this study did not take into account motion and T_2* effects. As a result, the value of R_2 (0.5) may not be optimal for in vivo studies though no apparent artifacts related to coil calibration were observed.

The recently developed coronary MRA using generalized auto calibrating partially parallel acquisition (GRAPPA) (10) employs VD sampling scheme, but achievable spatial resolution is limited due to additionally acquired calibration signals in the central k-space. Coronary MRA using sensitivity encoding (SENSE) (11) requires a separate scan for coil calibration. The separate coil calibration may result in wrong estimation of coil sensitivity due to the motion of coil and subject between calibration and imaging data acquisitions. The proposed method

is intermediate between the above two techniques in coil calibration, resolving the limitations mentioned above.

CONCLUSION

We have demonstrated a new method of combining extended data acquisition with parallel imaging for coronary artery imaging. This new technique offers the potential to enhance imaging efficiency and spatial resolution with no apparent motion-induced artifacts. The proposed extended acquisition strategy eliminates the need of separate scans for coil calibration, thereby reducing calibration errors for parallel imaging. Further investigations are necessary for more thorough systematic comparisons to establish the clinical efficacy of this new technique.

References

1. Bydder M, Larkman DJ, Hajnal JV. Generalized SMASH imaging. Magn Reson Med 2002;47(1):160–170. [PubMed: 11754455]
2. Pruessmann KP, Weiger M, Scheidegger MB, Boesiger P. SENSE: sensitivity encoding for fast MRI. Magn Reson Med 1999;42(5):952–962. [PubMed: 10542355]
3. Sodickson DK, Manning WJ. Simultaneous acquisition of spatial harmonics (SMASH): fast imaging with radiofrequency coil arrays. Magn Reson Med 1997;38(4):591–603. [PubMed: 9324327]
4. Sodickson DK. Tailored SMASH image reconstructions for robust in vivo parallel MR imaging. Magn Reson Med 2000;44(2):243–251. [PubMed: 10918323]
5. Sodickson DK, McKenzie CA. A generalized approach to parallel magnetic resonance imaging. Med Phys 2001;28(8):1629–1643. [PubMed: 11548932]
6. Griswold MA, Jakob PM, Heidemann RM, Nittka M, Jellus V, Wang J, Kiefer B, Haase A. Generalized autocalibrating partially parallel acquisitions (GRAPPA). Magn Reson Med 2002;47(6):1202–1210. [PubMed: 12111967]
7. Heidemann RM, Griswold MA, Haase A, Jakob PM. VD-AUTO-SMASH imaging. Magn Reson Med 2001;45(6):1066–1074. [PubMed: 11378885]
8. Jakob PM, Griswold MA, Edelman RR, Sodickson DK. AUTO-SMASH: a self-calibrating technique for SMASH imaging. SiMultaneous Acquisition of Spatial Harmonics. Magma 1998;7(1):42–54. [PubMed: 9877459]
9. McKenzie CA, Yeh EN, Ohliger MA, Price MD, Sodickson DK. Self-calibrating parallel imaging with automatic coil sensitivity extraction. Magn Reson Med 2002;47(3):529–538. [PubMed: 11870840]
10. Park J, McCarthy R, Li D. Feasibility and performance of breath-hold 3D true-FISP coronary MRA using self-calibrating parallel acquisition. Magn Reson Med 2004;52(1):7–13. [PubMed: 15236360]
11. Huber ME, Kozerke S, Pruessmann KP, Smink J, Boesiger P. Sensitivity-encoded coronary MRA at 3T. Magn Reson Med 2004;52(2):221–227. [PubMed: 15282803]
12. Paul D, Hennig J. Comparison of different flip angle variation functions for improved signal behavior in SSFP sequences. In: Proceedings of the 12th Annual Meeting of ISMRM, Kyoto, 2004, p2663.
13. Bieri O, Scheffler K. Generic eddy-current compensation in balanced steady-state free precession. In: Proceedings of the 12th Annual Meeting of ISMRM, Kyoto, 2004, p104.
14. Hansen PC. Rank-deficient and discrete ill-posed problems : numerical aspects of linear inversion. Philadelphia: Siam; 1998. xvi, 247 p.
15. Lin FH, Kwong KK, Belliveau JW, Wald LL. Parallel imaging reconstruction using automatic regularization. Magn Reson Med 2004;51(3):559–567. [PubMed: 15004798]
16. Shea SM, Kroeker RM, Deshpande V, Laub G, Zheng J, Finn JP, Li D. Coronary artery imaging: 3D segmented k-space data acquisition with multiple breath-holds and real-time slab following. J Magn Reson Imaging 2001;13(2):301–307. [PubMed: 11169838]
17. Stehning C, Nehrke K, Bornert P, Dossel O. ECG-triggered, Free Breathing Coronary MRA using Radial Balanced FFE with Intra-RR Motion Correction. In: Proceedings of the 12th Annual Meeting of ISMRM, Kyoto, 2004, p707.

18. Meyer CH, Hu BS, Nishimura DG, Macovski A. Fast spiral coronary artery imaging. Magn Reson Med 1992;28(2):202–213. [PubMed: 1461123]

19. Stehning C, Nehrke K, Bornert P, Dossel O. Continuous Epicardial Fat Suppression for Coronary MRA using Balanced FFE with Long Cardiac Acquisition Windows - A comparison of Two Techniques. In: Proceedings of the 12th Annual Meeting of ISMRM, Kyoto, 2004, p702.

20. Hargreaves BA, Vasanawala SS, Nayak KS, Hu BS, Nishimura DG. Fat-suppressed steady-state free precession imaging using phase detection. Magn Reson Med 2003;50(1):210–213. [PubMed: 12815698]

21. Deshpande VS, Shea SM, Laub G, Simonetti OP, Finn JP, Li D. 3D magnetization-prepared true-FISP: a new technique for imaging coronary arteries. Magn Reson Med 2001;46(3):494–502. [PubMed: 11550241]

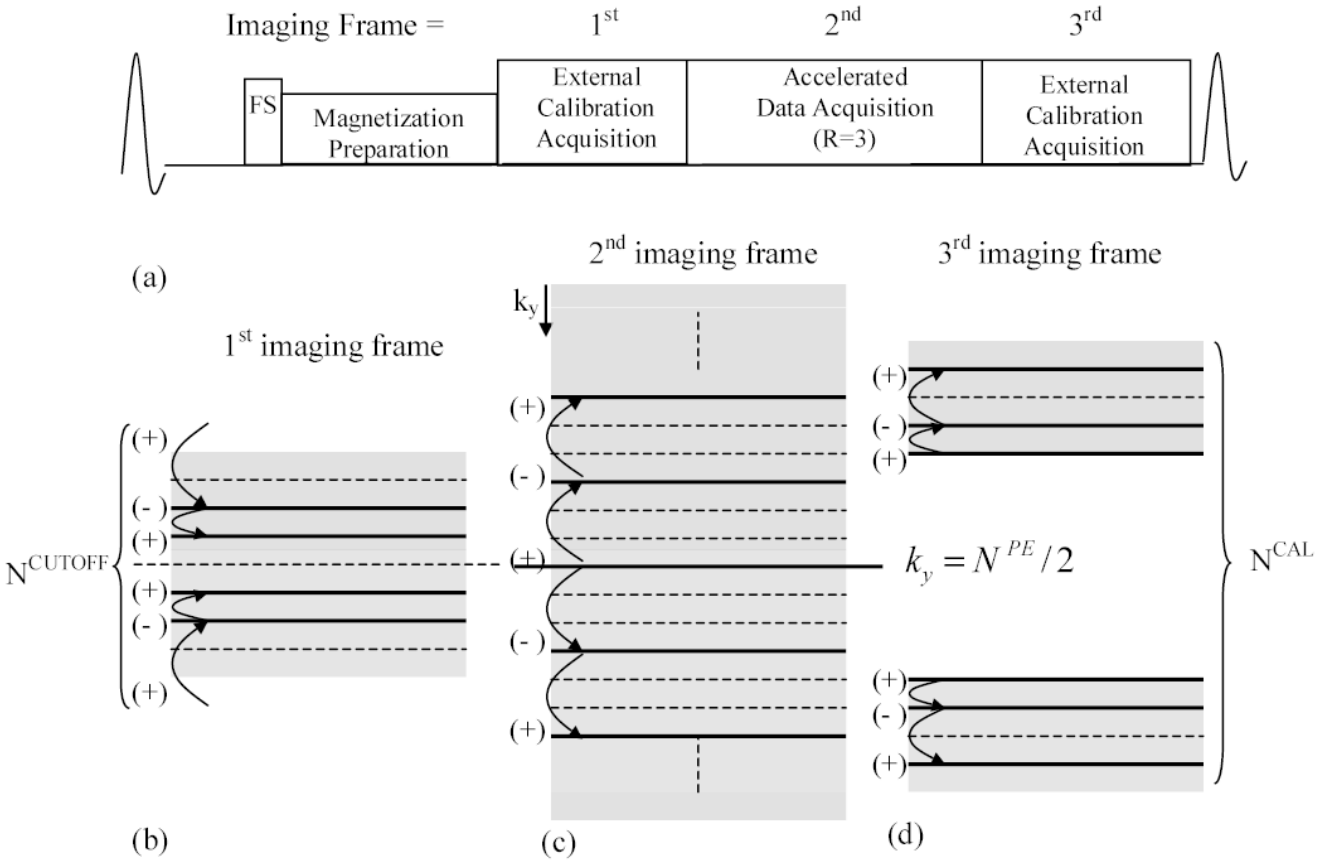

Figure 1.

A schematic of extended data acquisition over three imaging frames (a) with view ordering (b–d) (solid: measured line, dot: missing line, FS: frequency selective fat saturation pulse, k_y: PE index, *NPE*: total number of PE lines). (+) and (−) represent an alternating RF phase for the PE lines acquired in the neighborhood.

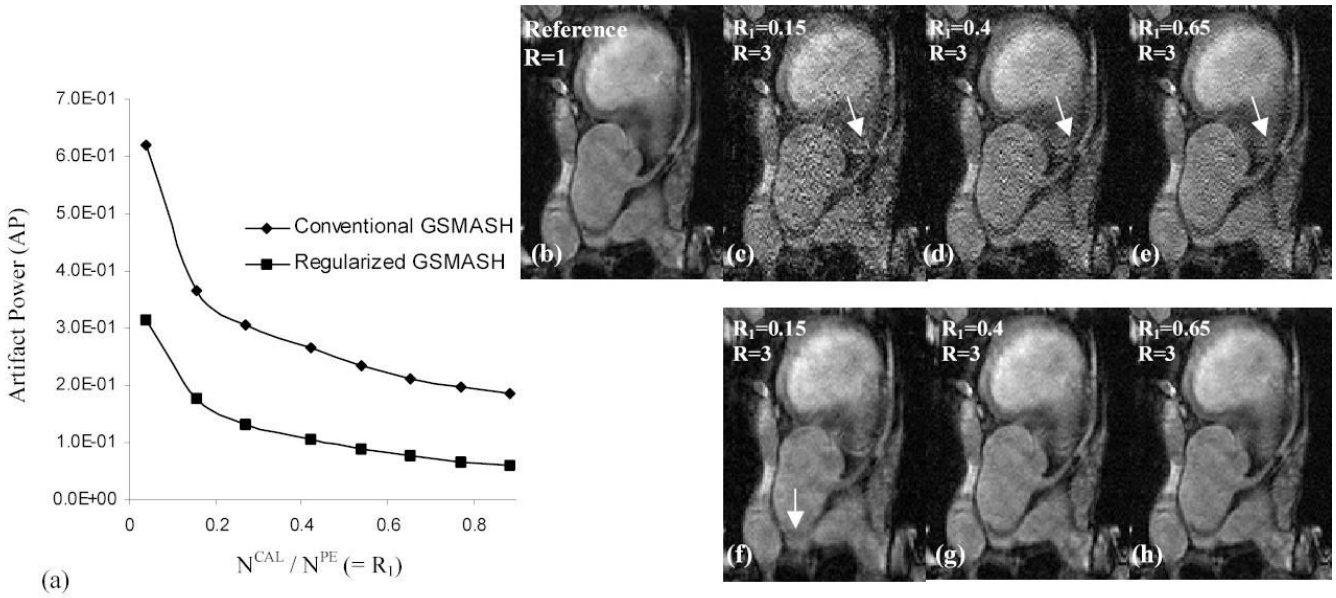

Figure 2.

Artifact power (AP) (a) and the corresponding images generated using conventional GSMASH (b–e) and regularized GSMASH (λ =5.0) (f–h) with the increase of R_1. Note that AP is rapidly decreased as R_1 reaches around 0.3, and noise is reduced by the regularization in GSMASH reconstruction.

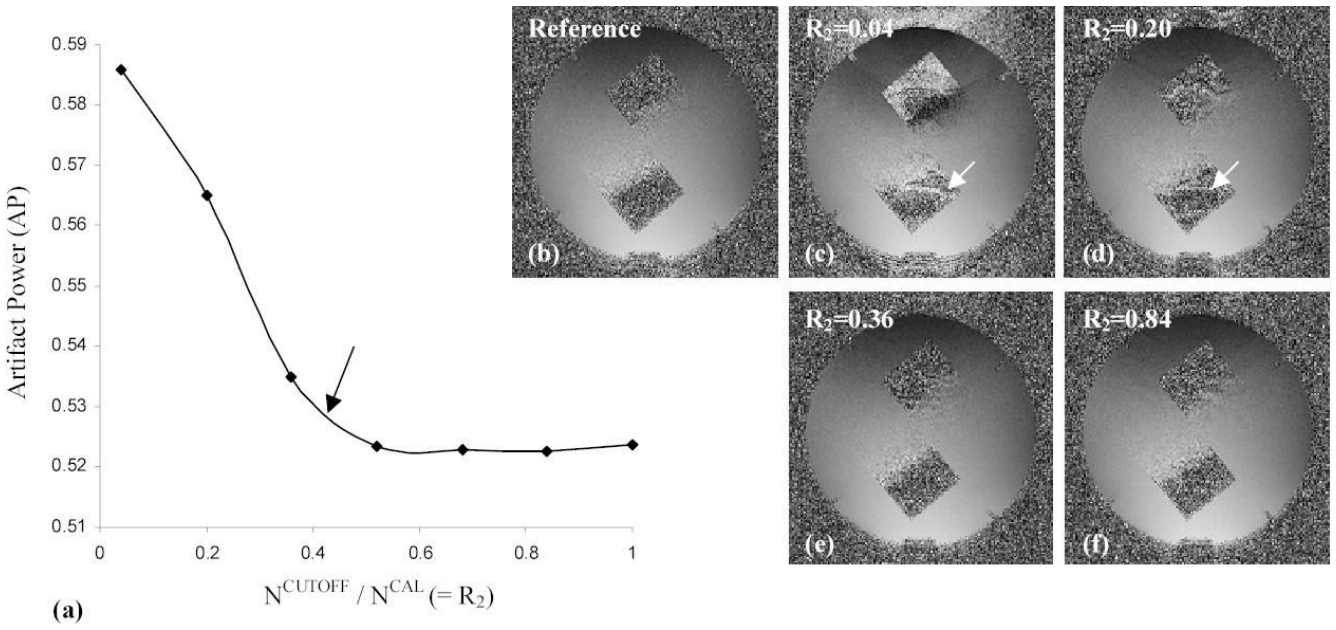

Figure 3.

Artifact power (AP) (a) and the corresponding coil sensitivity images (b–f) at different ratios of R_2 (R_1 = 0.4). Note that AP remains nearly the same at $R_2 > 0.4$ and signal discontinuity related artifacts in the coil sensitivity map are suppressed as R_2 is increased.

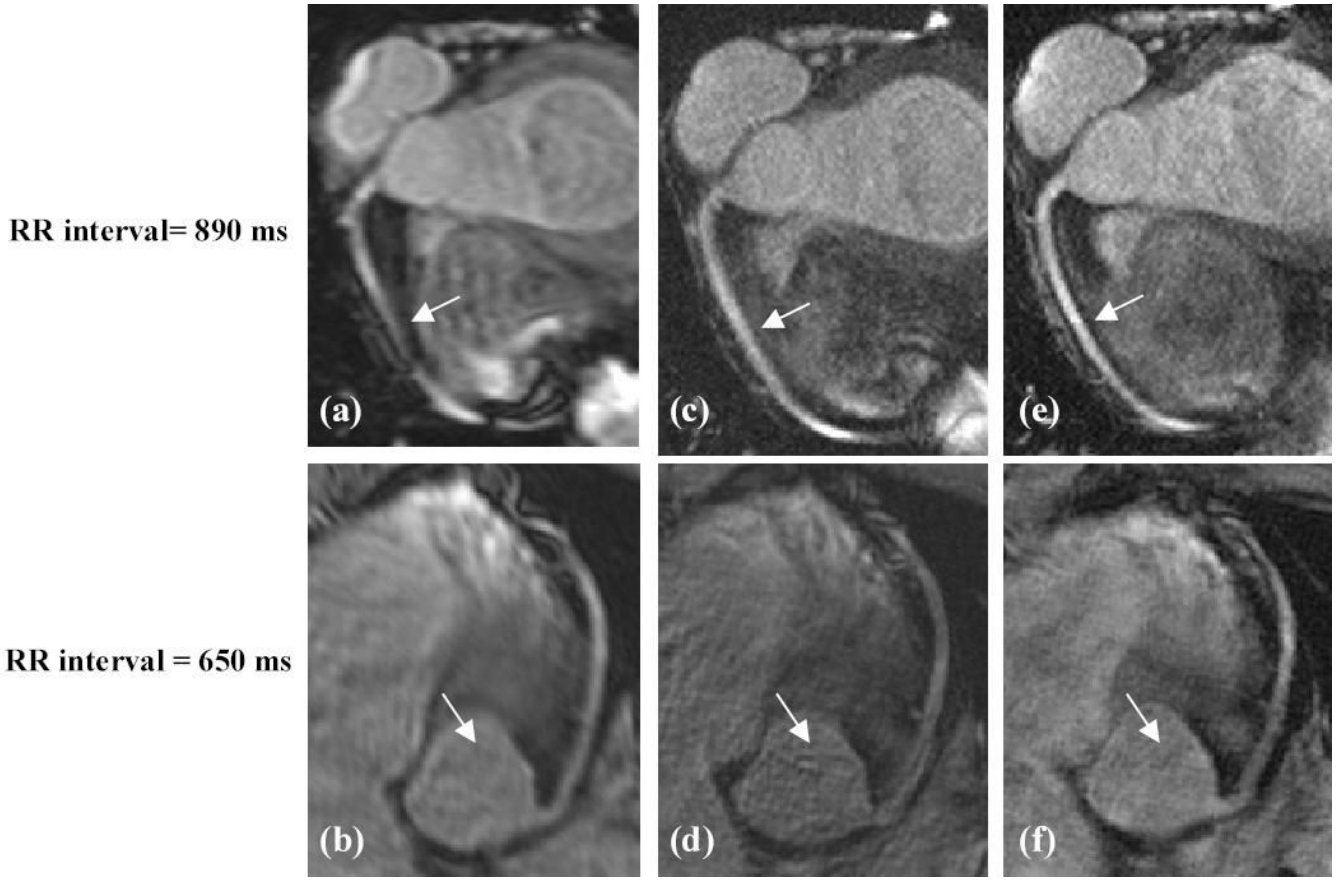

Figure 4.

Images generated using: (a–b) conventional acquisition with a short window (=127ms), (c–d) conventional acquisition with an extended window (=270ms), (e–f) and proposed acquisition (= 162 ms, R_1=0.4, R_2=0.5, R=3, λ =5.0). Note low resolution in (a–b), vessel blurring and motion artifacts in (c–d), and enhanced spatial resolution and reduced motion artifacts in (e–f). Also note that in extending acquisition window, motion artifacts are more severe with a short RR interval in (d) than with a long RR interval in (c).